Spatial and Temporal Variability in Ambient Mercury Concentrations

on the Colorado Front Range

A Thesis

Presented to

The Faculty of the Environmental Studies Program

Colorado College

In Partial Fulfillment of the Requirements for the Degree

Bachelor of Arts

By

Story Schwantes

May 2019

Dr. Lynne Gratz
Assistant Professor of Environmental Science

Dr. Rebecca Barnes
Assistant Professor of Environmental Science

Table of Contents

1. Abstract

Atmospheric mercury (Hg), an airborne heavy metal, can be deposited into aquatic and terrestrial systems, posing a risk to ecosystems and human health. It is therefore important to understand the sources, chemical cycling, and fate of atmospheric mercury. This study looks at total gaseous Hg (TGM) and total Hg (THg) concentrations collected at an urban near-road site in Colorado Springs, CO from June - August, 2016 and at a rural location in Rocky Flats National Wildlife Refuge, Louisville, CO, from June - August, 2018. Mercury concentrations at the two sites were significantly different from one another. The urban data set reveals a significant diurnal pattern, with hourly average TGM concentrations reaching a maximum at 3:00 MST (1.9 ± 0.3 ng/m^3) and minimum at 13:00 MST (1.6 ± 0.2 ng/m^3). In contrast, at the rural site we find that hourly-average concentrations peak at 13:00 MST (1.5 ± 0.1 ng/m^3) and are lowest at 6:00 MST (1.4 ± 0.1 ng/m^3). These diurnal Hg patterns are comparable to those found in other studies looking at urban/rural differences. Sources of Hg at both sites were also investigated. At the urban site, the data points to high TGM concentrations originating from local sources. Additionally, strong correlation between TGM and CO_2 suggests soil evasion as a potential Hg source. The rural site, on the other hand, does not appear to be influenced by nearby Hg point sources and reflects a typical background site.

2. Introduction

Atmospheric mercury (Hg) is an inorganic heavy metal that, at trace atmospheric levels, is considered non-toxic to inhale. Once deposited into aquatic and terrestrial ecosystems, Hg can undergo methylation and become the organic neurotoxin methylmercury (CH_3Hg). Methylmercury poses a health risk to both humans and animals. The neurotoxin bioaccumulates within food chains, meaning organisms absorb it faster than they can eliminate it. Within organisms that consume other organisms tainted by this form of mercury, the compound can quickly build to dangerous levels. In humans, Hg negatively affects the nervous and immune systems, and complications with reproduction and hormone imbalance have been found in animals exposed to significant quantities of Hg [1,2,3].

While direct exposure to high concentrations of Hg can result in problems with visual, auditory, and sensory systems, as well as affect motor function, the consequences of Hg exposure are most dangerous to fetuses exposed while in utero [4]. Mercury exposure in pregnant women has been linked to increased levels of neurological and developmental abnormalities in their offspring. One study estimates that children whose mothers are exposed to Hg while pregnant lose an average of 0.18 IQ points for every part per million (ppm) increase of Hg found the mother's hair [5]. This is a particular problem for coastal communities where fish is a main source of food, as fish efficiently absorb methylmercury into their tissues where it can bioaccumulate [6,7,8]. These health effects demonstrate the importance of understanding the sources, chemical cycling, and fate of atmospheric Hg.

Most atmospheric Hg comes from the combustion of Hg-containing substances. Natural sources include volcanoes and wildfires [1]. In the United States (US), the dominant source of anthropogenic Hg is power plants (mainly coal-fired). Coal-fired power plants release approximately 474 Mg/yr of Hg into the atmosphere, accounting for 21% of total global Hg emissions and 60% of emissions in the US. On a global scale, the largest anthropogenic source is small-scale and artisanal gold mining, emitting 838 Mg/yr [9]. Biomass burning as well as non-ferrous metal and cement production are other significant anthropogenic sources of atmospheric Hg.

All of the above sources are considered primary Hg emitters, inserting Hg directly into the environment from a lithospheric source [1]. Re-emission of Hg from aquatic and terrestrial surface reservoirs is a secondary source of atmospheric Hg and plays an important role in the global cycling of the toxin. This re-emission can occur through temperature increases affecting mercury vapor pressure, release of Hg through transpiration of vegetation stomata, surface moisture evaporation, and photochemical releases [10].

Once emitted, atmospheric Hg exists in three main forms. The first is gaseous elemental mercury (GEM), which has an atmospheric lifetime of ½-1 year [1]. Gaseous oxidized mercury (GOM) and particulate bound Hg (PBM), the two other forms predominant in the mercury cycle (Figure 1), are both assumed to be compounds of Hg^{2+} with short lifetimes of approximately one week. This brief lifetime, combined with the high water solubility of Hg^{2+}, makes Hg^{2+} much more likely than GEM to be deposited into terrestrial and marine environments, where it then may undergo methylation [1,4].

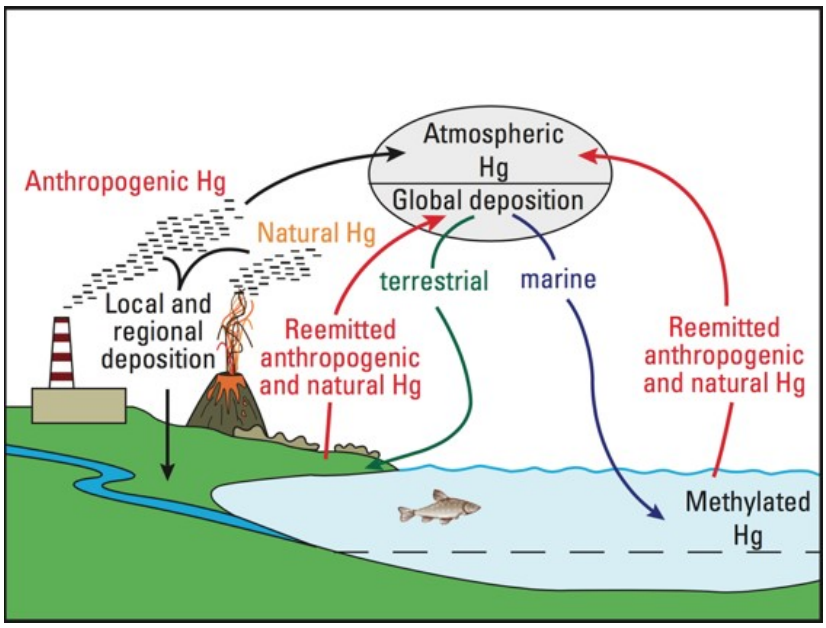

Figure 1: Basic mercury cycle [11].

Atmospheric Hg emissions have been steadily decreasing since the 1990s, largely due to sulfur (SO_2) emission controls initiated in the 1980s which also captured Hg [4]. Regulation passed in the 1990s addressing Hg in municipal and medical waste has also led to a decrease in atmospheric Hg emissions [12]. In 2011, the Mercury and Air Toxics Standards (MATS) rule was passed, which targeted coal- and oil-fired power plants by requiring Hg emission controls in place and effective within four years of the ruling [13]. Health benefits of decreasing atmospheric Hg levels identified in the initial MATS assessment included decreases in heart attacks, asthma, and premature death. These health benefits were initially estimated to be worth $36 to $90 billion; corresponding compliance costs to industry totaled $9.6 billion [14]. In December of 2018, the EPA released a new estimate of the costs and benefits of MATS, re-finding the quantifiable benefits to be worth only $4 to $6 million dollars [15]. As of now, MATS is still in place, but some advocates are concerned by what this reassessment could mean for the future of the rule itself as well as for environmental regulation in general [16,17].

In addition to the health effects and MATS ruling re-evaluation, the differences at urban and rural study sites make their own case for studying Hg. The increased complexity of emission sources, differences in surface characteristics, and the way in which urban factors can impact local meteorology make urban sites interesting to explore – especially when evaluated in context with rural sites absent of these [18]. Through urban/rural comparison, we can begin to understand how Hg and its cycling may be expected to differ at urban vs. rural sites. While other studies have looked at this urban-rural divide, Hg has not been studied as extensively in the western U.S. as it has in the more densely populated and industrialized eastern U.S. [19,20,21]. Sources of Hg in the western U.S. may differ from eastern sources due to differences in local industry and to lower population density. Colorado's mining history, significantly coal- and oil-combustion-fueled public energy sources, and the meteorological impact of the Rocky Mountains all make understanding Hg on the Front Range consequential. In this study, we examine atmospheric Hg at two contrasting urban/rural sites on the Colorado Front Range in order to better understand spatial and temporal patterns in atmospheric Hg concentrations in the region.

3. Methods

3.1. Site Descriptions

The urban site located in Colorado Springs is a Colorado Department of Public Health and Environment (CDPHE) air-monitoring site situated at the intersection of two major thoroughfares, Interstate 25 (north-south) and Highway 24 (east-west) (Figure 2, Urban site inset). Colorado Springs, population 464,474 (2,140.6/square mile) [22], rests

at the base of Pikes Peak and the Front Range of the Rocky Mountains. Two coal-fired power plants operate within 25 km of the urban study site. Martin Drake, with a 185-megawatt (MW) capacity [23], sits 800 meters southeast of the study site. Mercury scrubbers were installed there the year before measurement began, and SO_2 scrubbers were installed on the two units at the plant in February and September of 2016 [24]. Ray Nixon Power Plant (208 MW capacity), is located approximately 25 km southeast of the urban site [25]. Other inventoried Hg point sources within 30 km of the urban site include the Cripple Creek gold mine in Victor, CO and various small sources that emit less than 0.2 kg/yr (i.e. Colorado Springs Police Department, Colorado College, and Peterson Air Force base) [26]. Measurements at the urban site were taken from 6/15/16 to 10/20/16. This analysis focuses on data collected from 6/22/16 to 8/31/16 only in order to more directly compare with the rural/suburban site data from 2018. One 5-minute event was removed from the data analysis (8/31/16 12:35 – 40 MST) because it was determined to be an extreme outlier with total Hg concentrations approximately three times higher than the average concentration.

The rural site in this study was situated at the CDPHE air monitoring site in Rocky Flats National Wildlife Refuge (RFN), approximately 25 kilometers northwest of Denver and 14.5 km southeast of Boulder near the towns of Louisville and Superior (Figure 2, Rural site inset). RFN is a completed superfund site near a former nuclear weapons plant. It became a superfund site in 1989 and the plant shut down in 1994 [27]. At this rural site, data collection occurred from 6/20/18– 8/17/18.

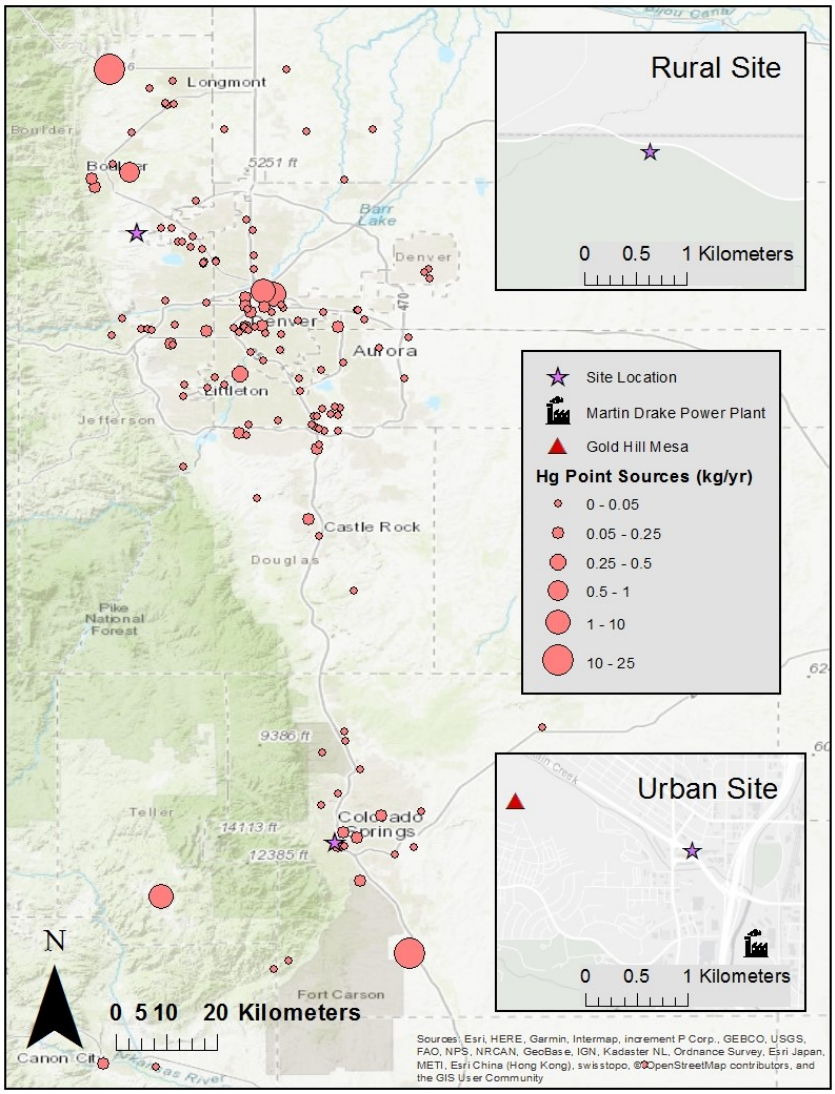

Figure 2: Study site locations and Hg point sources on the Colorado Front Range (point source indicators are not scaled to the size of emissions).

3.2. Mercury Measurements

3.2.A. Urban Site

At the urban site, we measured total gaseous Hg (TGM = GEM + GOM). Mercury was measured using the Tekran 2537A mercury vapor analyzer, which measures GEM. Ambient air was pulled into a 0.1-micron 47 mm PTFE particulate filter in a Teflon filter pack. At the urban site, air was filtered in order to reduce the risk of sample

line contamination by coarse particles stirred up by road maintenance occurring in the vicinity. The choice to utilize a filter here most likely has resulted in lower measured concentrations of THg due to both the removal of PBM and the suspected removal of some or all GOM that has been observed with filter usage in other studies [28,29]. Therefore, while we refer to this dataset as TGM, we acknowledge that our measurements may better reflect GEM. Air was pulled by a sample pump into the inlet and through a ¼" line heated to 100ºC at 7 L/min. We then pulled air off this main sample line at 1 L/min to a pyrolyzer, comprised of a glass tube containing quartz chips and quartz wool within a Lindberg Blue tube furnace which was continuously heated to 500ºC, the temperature at which GOM is desorbed and converted entirely to GEM [30,31]. Downstream of the pyrolyzer, 5-minute integrated measurements of GEM were detected by atomic fluorescence spectrophotometry (CV-AFS) with the Tekran 2537A.

3.2.B. Rural Site

The rural site measured total atmospheric Hg (THg = GEM + GOM + PBM) and had a slightly different inlet setup: instead of a filtered inlet, this sample line was fitted with a glass elutriator that excluded particulate matter above 2.5 microns. Air then was pulled through a heated main sample line (100ºC) and the sample pulled off the main line at 1 L/min to the pyrolyzer which was heated to 650ºC. Studies have shown that between 500 and 1000ºC there is no statistically significant difference in desorption amounts [32], and thus we assume that at both the urban and rural sites our method converted all oxidized Hg to GEM despite the different pyrolyzer temperatures. After the pyrolyzer phase, the same steps were followed as at the urban site.

We acknowledge here that there were slight differences in the Hg sampling methods between the two sites analyzed. First, the data sets were taken approximately two years apart. Second, they tracked slightly different forms of atmospheric mercury; the 2016 urban site observed the total gaseous Hg (TGM) concentrations, while the 2018 rural site tracked total atmospheric Hg (THg) which is TGM plus particulate-bound Hg (PBM). At the rural site, we also measured speciated Hg, and found the mean Hg^{2+} concentration to be 0.036 ± 0.073 ng/m^3, or 2% of the THg measurement, meaning we were mostly measuring Hg^0. While not a perfect pairing, we can still learn about patterns and sources of Hg from comparing the two data sets. Similar ancillary data between the sets allows for an even better comparison and exploration into the mechanisms driving observed patterns.

3.3. Ancillary Data

CDPHE provided continuous 1-minute measurements of temperature, wind direction/speed, and relative humidity at each site. At the urban site, carbon monoxide (CO) and SO_2 were measured using Thermo Scientific 48i and Teledyne API 100E analyzers, respectively. CDPHE also provided ozone (O_3) measurements at the rural site, measured with the Teledyne API T400 analyzer. To match our Hg data, all ancillary data was averaged to 5-minute intervals. We also measured carbon dioxide (CO_2) at both sites using a LiCor LI-840A continuous CO_2/H_2O analyzer. At the urban site, we made 1-minute measurements; at the rural site, we made 2.5-minute measurements. We then computed 5-minute averages for equivalent comparison.

3.4. Data Analysis

Data analysis was done predominantly using IBM SPSS 24.0 and Microsoft Excel, with wind roses created using Matlab vR2014b. Pearson correlation coefficients were found for all data at both sites, and p-values were calculated. Independent samples t-tests were used to compare all means. For all analyses, a p-value equal to or less then 0.01 was considered statistically significant.

4. Results/Discussion

4.1. Colorado Springs Highway 24 Site: Urban

The study average concentration of TGM at the urban location (1.7 ± 0.3 ng/m^3) is above the range of expected background concentrations for the Northern Hemisphere (1.3 - 1.6 ng/m^3) [33]. The data shows a range of TGM concentrations spanning from 1.0 ng/m^3 to 3.5 ng/m^3, however 90% of the data fell between 1.4 and 2.2 ng/m^3 (Figure 3a).

We also see elevated levels of the other chemical data taken at the urban site. Sulfur dioxide levels are high (4.0 ± 1.4 ppb), consistent with the collection site's proximity to a coal-fired power plant and two major roadways, as SO_2 is emitted through the combustion process [34]. Carbon dioxide (422 ± 21 ppm) is well above the 2017 global average of 405 ppm [35]. Considering this site's location near a coal-fired power plant and two major roadways, with CO_2 emitted during both coal and automobile fuel combustion, elevated concentrations are again not surprising [36]. Yet another product of combustion, CO, has an average concentration (0.29 ± 0.16 ppm) more than double the Northern Hemisphere background levels found in other studies [37,38].

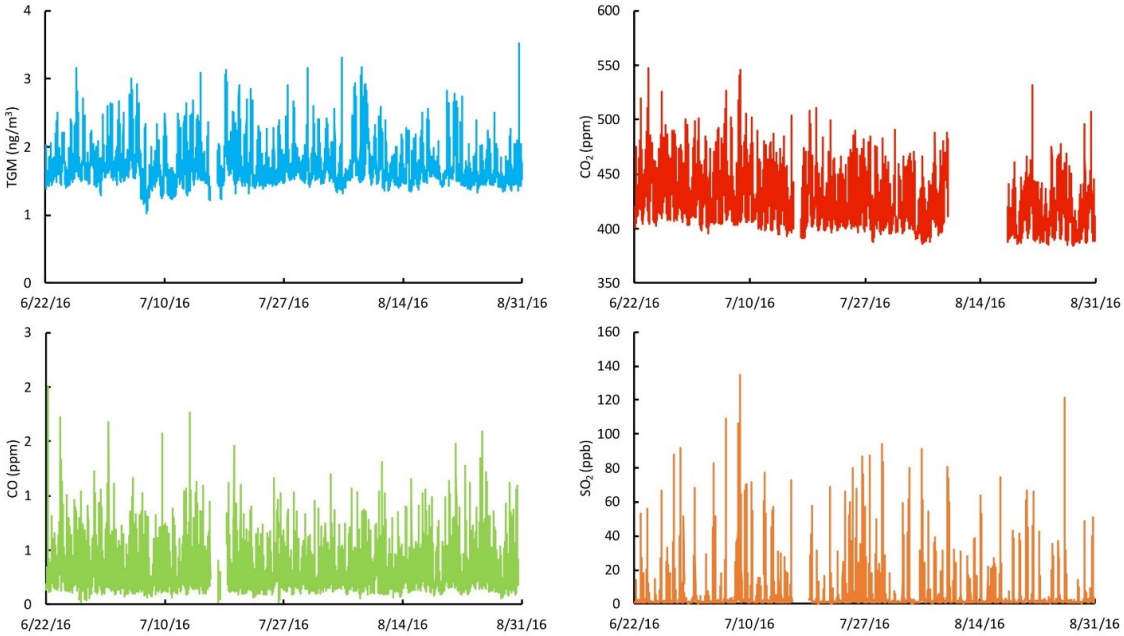

Figure 3: Time series of (a) TGM, (b) CO_2, (c) SO_2, and (d) CO concentrations at the Colorado Springs urban site.

	TGM (ng/m^3)	**SO_2 (ppb)**	**CO (ppm)**	**CO_2 (ppm)**
Mean	1.7	4.0	0.29	422
Median	1.6	1.4	0.24	419
Std. Deviation	0.30	8.4	0.16	21
Minimum	1.0	0.02	0.01	384
Maximum	3.5	135	2.0	548
25th percentile	1.5	1.1	0.17	406
75th percentile	1.8	2.5	0.35	435
N	19842	18701	18606	17373

Table 1: Summary statistics for TGM, SO_2, CO, and CO_2 at the urban site in Colorado Springs.

Night and day at both sites were defined with 7:00-19:00 MST considered *day*, and the remaining 12 hours defined as *night*. The average daytime TGM concentration (1.6 ± 0.2 ng/m^3) is significantly lower than the night average (1.8 ± 0.3 ng/m^3) (Table 2). A distinct diurnal pattern can be seen in the average hourly data, with an average hourly TGM maximum of 1.9 ± 0.4 ng/m^3 observed at 4:00 MST (night) and minimum of $1.6 \pm$

0.1 ng/m^3 at around 13:00 MST (day) (Figure 4a). This diurnal TGM pattern has been observed in other studies at urban sites in North America and is generally attributed to high surface concentrations of Hg which are diluted when the boundary layer is higher making some vertical mixing possible [20,39]. This is most likely what is happening at the urban site we surveyed, as a mixing height analysis done on the data showed a pattern in which the boundary layer was twice as high in the evening as in early morning [40].

	TGM (ng/m^3)	**SO_2 (ppb)**	**CO (ppm)**	**CO_2 (ppm)**
Day Mean	1.6	6.0	0.31	417
Day Std. Deviation	0.16	11	0.16	19
Night Mean	1.8	1.8	0.26	428
Night Std. Deviation	0.30	3.7	0.16	22

Table 2: Night/Day averages and standard deviations of chemical data at the urban site.

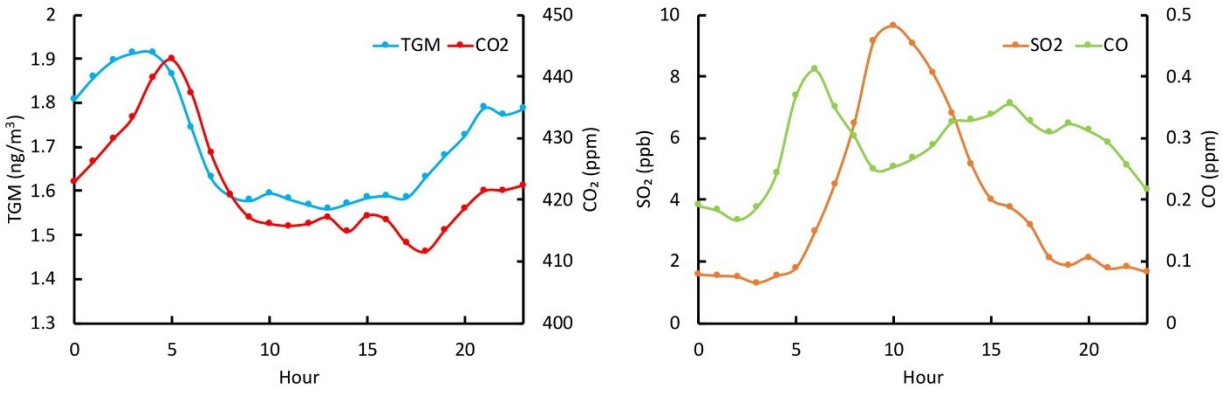

Figure 4: (a) Hourly averages of TGM and CO_2 and (b) hourly averages of SO_2 and CO at the urban site.

Sulfur dioxide concentrations see a peak at 10:00 MST and reach a minimum around 3:00 MST, a fairly dissimilar diurnal pattern to that of TGM (Figure 4b). This relationship between SO_2 and TGM was important in ruling out Martin Drake and Ray

Nixon power plants as a source of Hg. There is little correlation between SO_2 and TGM ($r = -0.08$) which we would expect to see if the source of TGM were the power plants (Table 3). In addition to correlation with SO_2 we would expect to see high TGM concentrations coming from the SE where the power plants are located relative to the site. A wind analysis showed that, during the period of study, wind came from the northwest (292.5º-337.5º) 27% of the time, and from the southeast (112.5º-157.5º) 19% of the time. The NW direction also sees the highest mean TGM concentration (1.8 ± 0.3 ng/m^3), while the SE winds brought a TGM average statistically significantly lower (1.6 ± 0.2 ng/m^3) with the second-lowest concentration of the eight directions analyzed (Figure 5). Though it was initially suspected that Hg in the urban area would be coming from the nearby power plants, the data makes clear that they are not a significant source of Hg for this measurement site. A local source of TGM is not ruled out, however, as the highest TGM concentrations are associated with low wind speeds (< 4 mps), indicating that another nearby source(s) is emitting TGM (Figure 5).

	TGM	**SO_2**	**CO**	**CO_2**	**Temp**	**RH**	**WS**
TGM	1	-0.08	0.18	0.53	-0.40	0.43	-0.38
SO_2	--	1	0.05	0.23	0.18	-0.10	0.23
CO	--	--	1	0.43	0.07	-0.05	-0.09
CO_2	--	--	--	1	-0.18	0.18	-0.27
Temp	--	--	--	--	1	-0.87	0.40
RH	--	--	--	--	--	1	-0.32
WS	--	--	--	--	--	--	1

Table 3: Pearson correlation coefficients for chemical and meteorological data at the urban Colorado Springs site. All values are statistically significant to $p<0.01$.

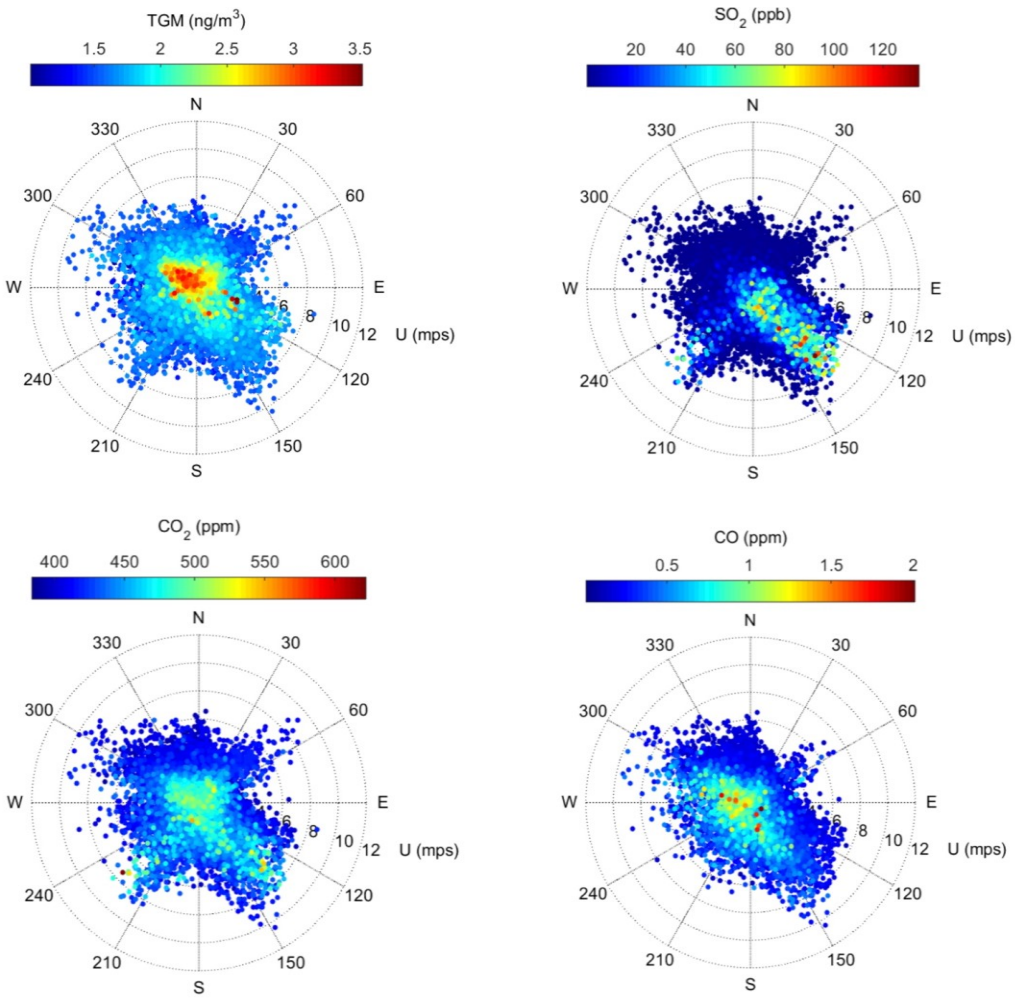

Figure 5: Polar plot of (a) TGM, (b) SO_2, (c) CO_2, and (d) CO at the urban site.

A strong correlation exists between TGM and CO_2 ($r = 0.528$) and the diurnal patterns follow each other closely, with CO_2 peaking at 5:00 MST and reaching an average minimum at 18:00 MST (though it is consistently low from 9:00 MST on) (Figure 4a). Assuming a normal daytime photosynthesis/nighttime respiration cycle and considering the location's proximity to major sources of combustion, this diurnal pattern is expected. Other studies have explored strong relationships between CO_2 and TGM through the lens of soil evasion which may play a role in the TGM seen at the urban site [41]. First, road construction was being conducted nearby throughout the duration of the sampling period, and the soil tilling involved in road work has been shown to be

associated with higher TGM concentrations [42]. Secondly, Gold Hill Mesa is located approximately 290º NW of the sampling site. When wind was blowing from this direction, we observed the highest average TGM concentrations and the highest CO_2 concentrations (Figure 5). This brings up the possibility of soil evasion of TGM from the Cripple Creek Mine tailings at that site, which may contain gold particles that have collected Hg and are re-evading it back into the atmosphere [43]. Cripple Creek Mine was also known to use Hg in the mining process [44].

Carbon monoxide concentrations trace a diurnal pattern which correlates with nearby emissions from vehicles and heavily corresponds with expected traffic patterns (Figure 4b). A 6:00 MST morning peak and 16:00 MST afternoon peak, in addition to generally elevated concentrations much of the late afternoon/evening, support the theory that observed CO comes predominantly from vehicle emissions, but we see little correlation between CO and TGM ($r = 0.18$) (Table 3).

July 24th is a 24-hour period that gives an example of the patterns found above. This day was chosen to illustrate that the patterns discussed above occur regularly throughout the study. The selected day is a typical summer day in Colorado Springs, CO, sunny with an afternoon thunderstorm. The average TGM concentration on 7/24/16 was 1.6 ± 0.2 ng/m^3. The patterns of each of the four chemical compounds show more variability during daytime hours, but generally follow the same diurnal patterns as are seen in the larger data set (Figure 6). TGM concentrations are significantly higher during the night, and peak during the early morning prior to sunrise. Carbon dioxide once again follows a pattern very similar to TGM, peaking in the early morning and falling off after that, with an average of 417 ± 12 ppm. The diurnal pattern of SO_2 appears the most

different from the average pattern of the full data set, showing, instead of only one midday peak, two peaks on either side of midday, with one major increase occurring at 18:05 MST while wind is coming from 140º, indicating the source may be the power plants. The average SO_2 concentration is extremely close to that of the full data set, at 3.8 ± 6.2 ppb. The correlations between these elements also mirror that of the full summer. Sulfur dioxide and CO see very weak correlations with TGM (r = -0.1 and r = 0.05 respectively), while CO_2 shows a strong correlation (r = 0.66). Wind direction analysis shows that the most common wind direction is the northwest (31% of the time), which also has the highest average TGM and CO_2 concentrations, the same pattern seen in the broader data set.

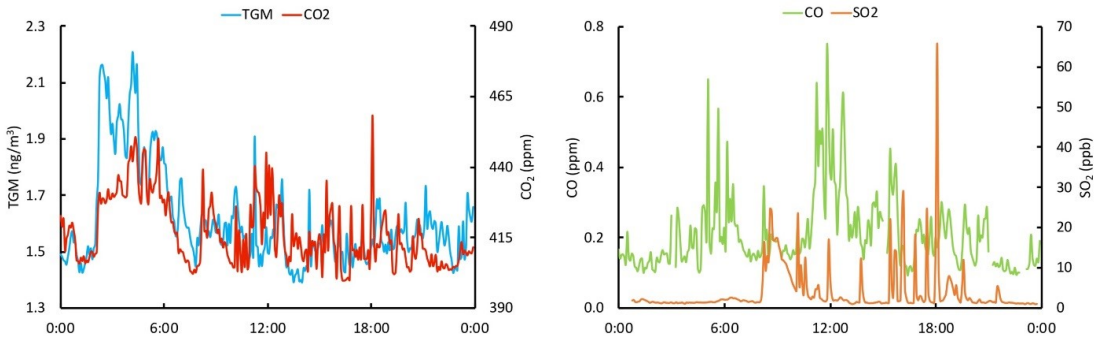

Figure 6: Time series graphs of (a) TGM and CO_2 and (b) CO and SO_2 data for 7/24/16 at the urban site.

4.2. Rocky Flats National Wildlife Refuge Site: Rural

Average THg concentrations (1.5 ± 0.1 ng/m^3) at the rural location are within the expected range for the northern hemisphere background (Figure 7a) [33]. At the rural site, we see a very weak diurnal pattern (Figure 8). The slight pattern that does exist shows an increase in THg during the day with a peak of 1.5 ± 0.1 ng/m^3 around 13:00

MST, with concentrations falling slightly during the night and early morning reaching a low of 1.4 ± 0.1 ng/m^3 at 6:00 MST before again beginning to rise.

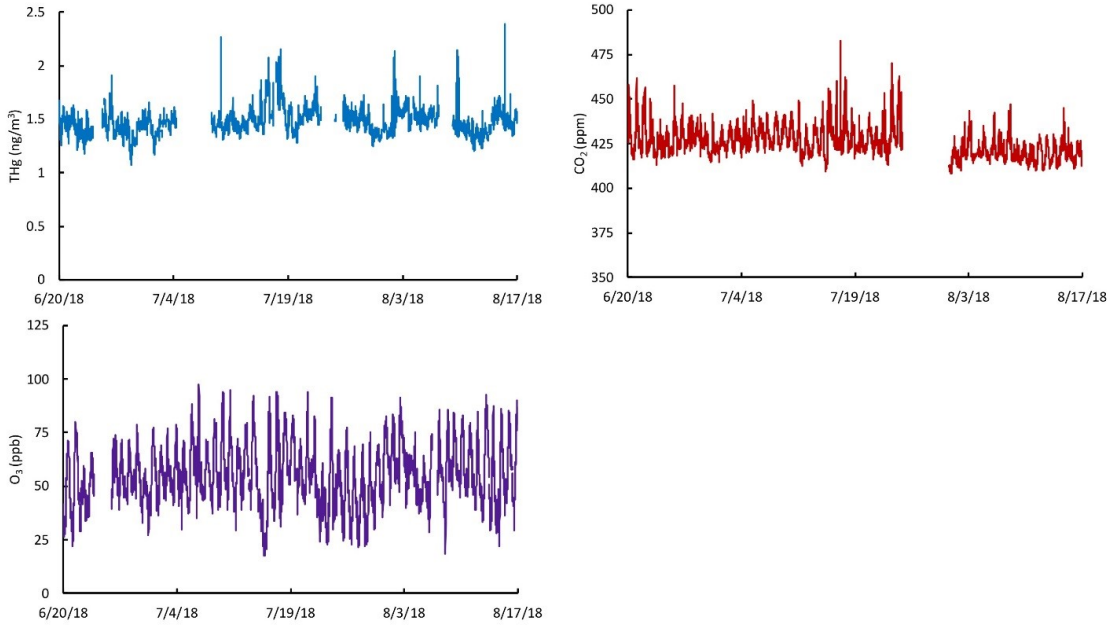

Figure 7: Time series of (a) TGM, (b) CO_2, (c) O_3 concentrations at the Rocky Flats rural site.

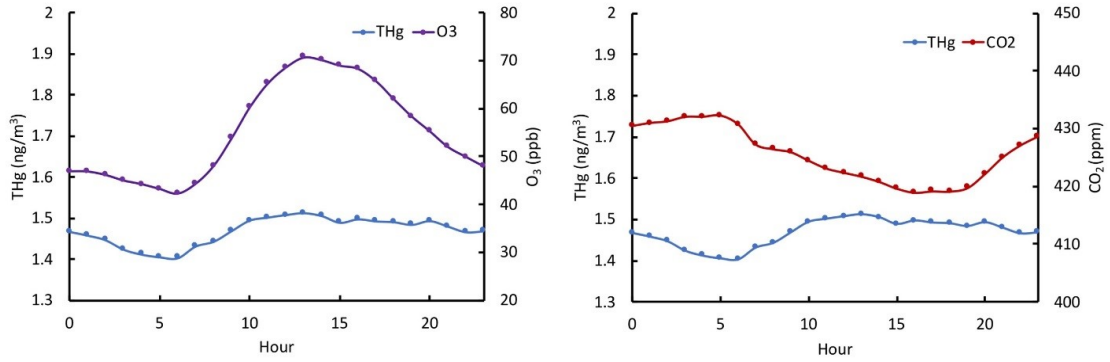

Figure 8: Hourly averages of (a) O_3 and THg at the rural site and (b) CO_2 and THg at the rural site.

	THg (ng/m^3)	O_3 (ppb)	CO_2 (ppm)
Mean	1.5	55	425
Median	1.5	54	424
Std. Deviation	0.1	14	8
Minimum	1.1	18	408
Maximum	2.4	98	483
25th percentile	1.4	46	420
75th percentile	1.5	65	430
N	12410	15837	15168

Table 4: Summary statistics for THg, O_3, and CO_2 at the rural site, Rocky Flats National Wildlife Refuge.

The variation between daily average highs and lows is far subtler at the rural site. It follows a not-uncommon pattern found at rural/remote sites where Hg peaks during midday, and minimum concentrations are seen during the early morning/night time [10,18,45,46]. This diurnal pattern has been attributed to the increase in photochemical release during the day along with increased evaporation from sources that may contain Hg, and an increase in ground surface flux of THg [20,45]. The rural study site was predominantly covered in native grasses and studies have shown that grass as a surface sees a small amount of diurnal Hg flux; this aligns with our findings [18].

The mean CO_2 concentration is 425 ± 8 ppm, and the average diurnal pattern is again as expected, with a maximum of 432 ± 8 ppm at 5:00 MST right around/before sunrise and a daily low near 419 ± 4 ppm at 16:00 MST (Figure 8b). Carbon dioxide and THg also seem to follow an opposite diurnal pattern. The two chemicals are not significantly correlated which aligns with their distinct diurnal patterns and suggests they do not share a common source ($r = 0.01$, $p = 0.81$).

	THg	O_3	CO_2	Temp	RH	WS	Barometric Pressure
THg	**1**	**0.21**	0.01	**0.16**	**0.14**	**-0.07**	**0.25**
O_3	--	**1**	**-0.48**	**0.78**	**-0.7**	0.03	**-0.11**
CO_2	--	--	**1**	**-0.32**	**0.31**	**-0.14**	0.06
Temp	--	--	--	**1**	**-0.83**	0.06	**-0.27**
RH	--	--	--	--	**1**	-0.05	**0.43**
WS	--	--	--	--	--	**1**	**-0.12**
Barometric Pressure	--	--	--	--	--	--	**1**

Table 5: Pearson correlation coefficients for chemical and meteorological data at the rural site. Bolded values are statistically significant to $p<0.01$.

The mean O_3 concentration at this site, 55 ± 14 ppb, is above the normal range for background levels (30-50 ppb) [47]. Ozone is slightly positively correlated with THg ($r = 0.21$) and they share a similar diurnal pattern (Figure 8a). The lowest concentrations generally occur at 6:00 MST and peak during the early afternoon, around 13:00 MST. This is logical considering the photochemical activity essential to O_3 creation and the assumed influx of O_3 precursors like NO_x and CO produced by sources expected to be more abundant during the daytime hours (e.g. vehicles). High concentrations of O_3 are predominantly present when the wind comes from the northeast (Figure 9c). This could be due to the prevalence of oil and natural gas production happening along the I-25 corridor north of Denver, which produces the necessary O_3 precursors [48].

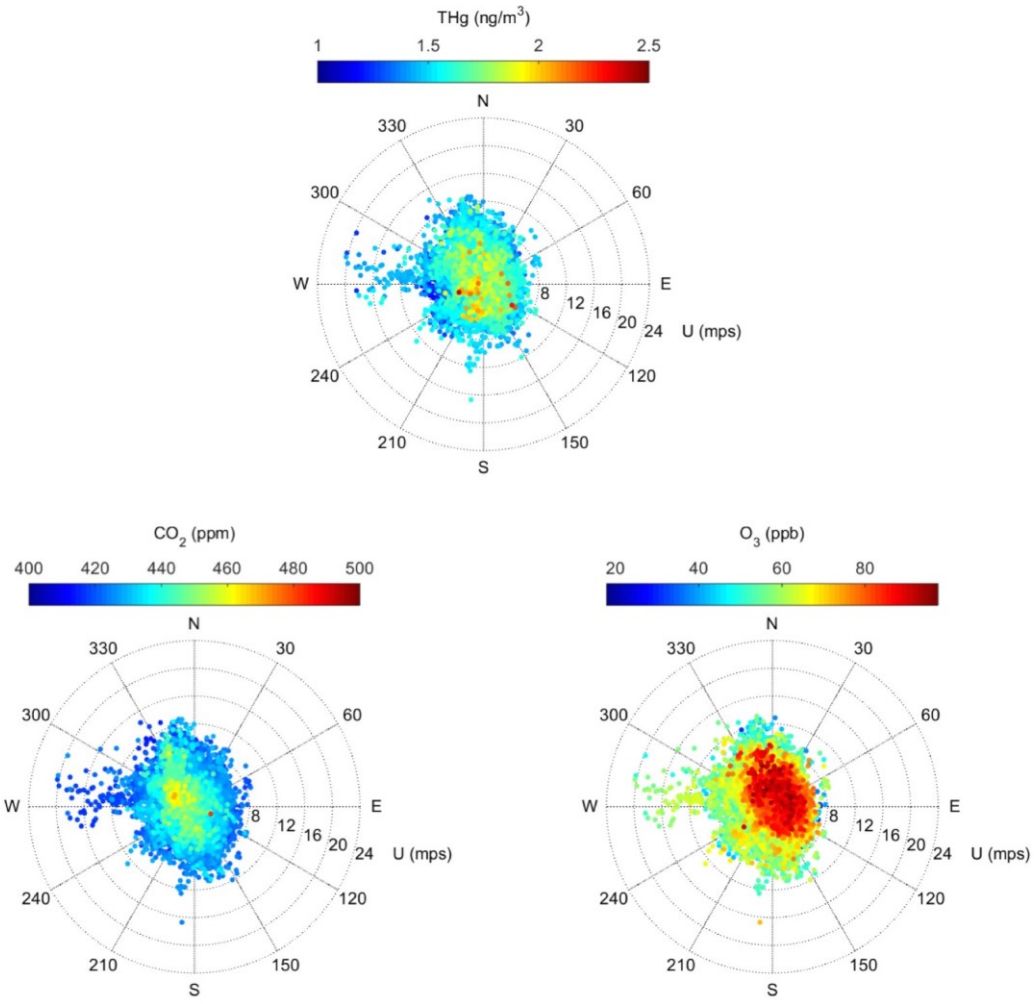

Figure 9: Wind roses for (a) THg, (b) CO_2, and (c) O_3 at the rural site.

The results of a wind direction analysis showed that the highest mean concentrations of THg are coming from the east-southeast (1.50 ± 0.09 ng/m^3 and 1.49 ± 0.12 ng/m^3, respectively). These averages are significantly higher than concentrations measured in the presence of wind prevailing from any other direction, though the absolute difference between the highest and lowest concentration is only 0.06 ng/m^3 demonstrating minimal differences in concentration as a function of wind direction. While the highest average concentrations are associated with winds coming from the east-southeast, the direction of Denver where there is a greater density of Hg point

sources (Figure 2), the predominant wind direction during this summer study period is north-northwest (33% of the time compared to only 19% for easterly and southeasterly winds) (Figure 9). This implies that Denver area sources have a small impact on the site, but they do not play a significant role because of the prevailing wind directions.

Barometric pressure has the strongest correlation with THg ($r = 0.25$), but this too is technically weak, and indicates that only ~6% of the variation in pressure explains THg variation. Regions of high atmospheric pressure move air toward the ground, and what we could be seeing is evidence of influence from the upper-tropospheric pool of Hg^{2+} wherein, as a high-pressure system moves into the region, we see air rich in Hg being moved down to the surface. Judging by the r-value, however, this may not be a frequent occurrence, at least during this study's summertime sampling period [1,4,49]. The general diurnal trend of barometric pressure shows a diurnal pattern with a decrease during the daylight hours, opposite of the increase in THg seen during that period (Figure 10). Past studies have attributed the relationship between these two trends to the decrease in barometric pressure allowing off gassing of THg from the soil surface during the daytime, though the relationship with CO_2 described above doesn't suggest a major surface source [50].

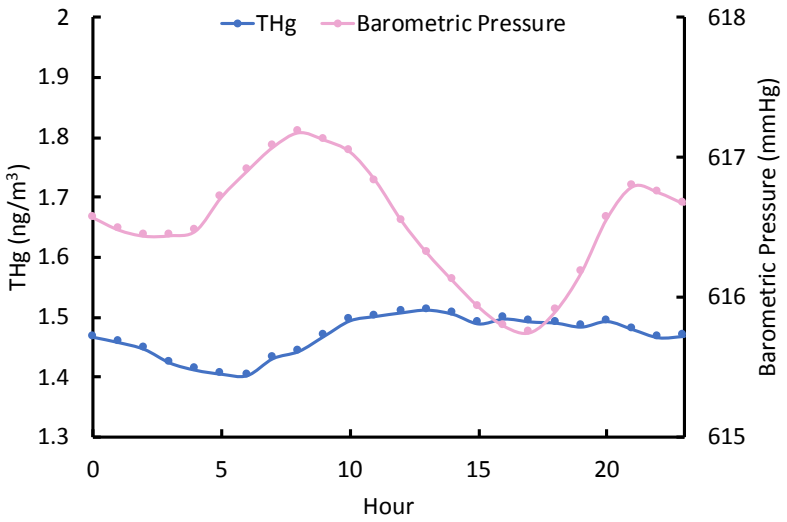

Figure 10: Hourly averages of THg and Barometric Pressure at the rural site.

4.3. Comparison between Urban and Rural Locations

The urban and rural sites' Hg concentrations are significantly different from one another. While studies have shown that total atmospheric Hg concentrations are decreasing worldwide (~1-2% per year), this amount is not enough to allow attribution of the Hg decrease between this study's 2016 and 2018 observation periods to globally seen decreases [12]. This means that the urban site is in fact experiencing Hg levels above background. The urban site also has significantly higher night and day average Hg concentrations than the rural site. The magnitude of diurnal change is also much greater at the urban area, with a total change from day to night of 0.2 ng/m^3 (Table 2). This change is negligible at the rural site with a total difference of only 0.04 ng/m^3 (Table 6). This difference between sites is due to the influx of Hg from local point sources that the urban site experiences and which are not seen at the rural site.

	THg (ng/m^3)	O_3 (ppb)	CO_2 (ppm)
Day Mean	1.5	60	424
Day Std. Deviation	0.1	14	8
Night Mean	1.5	48	428
Night Std. Deviation	0.1	11	8

Table 6: Variance and Night/Day averages of chemical data at the rural site.

The atmospheric soundings which we used to help explain the diurnal pattern at the urban site are from Stapleton, CO. This location is actually closer in proximity to the rural than to the urban site, implying that the same diurnal differences in mixing height we determined for the urban site would likely also be applicable to the rural one had we generated them for the 2018 study. If diurnal changes in mixing height were the only factor driving Hg concentrations, one might expect to see similar timing of nighttime and daytime peaks at the two sites. Supposing both locations underwent the same changes in boundary layer height at those times, it is possible that, because of the fewer point sources at the rural site, the movement of the boundary layer does not significantly affect ambient concentrations in the manner observed at the urban site. At the urban site, the increased daytime boundary layer height dilutes the Hg concentrations; when it compresses at night we see an increase in concentrations because of reduced vertical mixing. At the rural site, we can explain the diurnal pattern by higher nighttime deposition in the stable nocturnal boundary layer; surface emissions during the day increase concentrations again. Other studies have noted these patterns and included these explanations for the above diurnal patterns [20,39,51].

Mean CO_2 concentrations are also significantly different between sites. Despite the urban site having more potential local CO_2 emission sources, the rural site has a higher concentration. These average increases may be attributed to increases on a global scale that occurred during the two years between collection, as this increase does not appear to be related to THg concentrations (Tables 1 & 4) [52].

In comparing the two sites, it is clear that they have different sources of Hg. At the rural site, we do not see exceptionally elevated THg concentrations. There are no high correlations between THg and other data, both chemical and meteorological. And the magnitude of the diurnal pattern is small, though night and day are significantly different. Combined, these findings indicate that the rural site is not, on average, influenced by nearby point sources in the greater Denver and Boulder area, and what we are seeing are background patterns and expected regional THg concentrations.

It is surprising that we do not see more influence from the many point sources in the greater Denver area. The wind direction analysis discussed in section 4.2 indicated that the prevailing winds at the rural site are from the north-northwest, limiting the impact of point sources from the Denver metropolitan area southwest of the measurement site. It may also be attributable to the fact that the urban site is in very close proximity to multiple Hg sources, and the rural site is located at a great enough distance from point sources that the influence isn't detectable. Observations and analyses at the urban site point to an extremely local influence, which we do not see at the rural site.

The urban site shows Hg above average background levels. A few significant correlations with other data could indicate possible sources. Carbon dioxide and TGM have the highest correlation, suggesting they may have a similar source. In the wind

direction analysis, CO_2 and TGM also see their two highest average concentrations coming from the same directions: west and northwest. This is both the direction of U.S. Route 24 and Gold Hill Mesa. In the absence of additional data, it is difficult to conclude with any certainty that there is a specific source contributing to the high TGM concentrations seen at the urban site, but it is clear that there are discernable differences in the magnitude and temporal patterns between the urban and rural measurement sites.

5. Conclusion

This study validated the expectation of diurnal Hg concentration patterns at each site, considering their urban and rural natures, but its results also gave insight into potential origins for the excess Hg at the urban site. At that site, diurnal changes in the boundary layer height likely played a particularly important role in the ambient Hg patterns observed there. Mercury's positive correlation with CO_2 and inverse correlation with wind speeds further indicate that there is potentially a local soil source of Hg impacting the urban location concentrations. Also at the urban site, two nearby power plants were determined not to be a significant source of TGM. This finding is consistent with the reported installation of emission controls at both facilities prior to the study. On average, the rural site does not appear to be strongly impacted by nearby point sources in the greater Denver and Boulder areas which may be the result of prevailing wind patterns. Contrasting the results of the data at the rural and urban sites helped establish and quantify a typical background site on the Colorado Front Range, providing future studies a regional baseline. This study adds to the understanding of how Hg concentrations are potentially impacted at urban versus rural sites in a region not

previously extensively studied. Finally, it points to the value of continued investigation of the cycling of Hg on the Colorado Front Range.

6. Acknowledgements

Dr. Lynne Gratz is an inspiration. I want to thank her for the opportunity to do research and create this thesis, for being a true mentor, for insightful and precise feedback, and for her endless generosity, kindness, and friendship. I also want to thank my second reader Dr. Becca Barnes who has a spectacular presence and an abiding sense of good humor. Sincerely grateful for the contributions of Dr. Seth Lyman, Chris Eckley, Erick Mattson, Darren Ceckanowicz, Sharon Johnson, and Melissa Tiang. And thanks for my lovely and completely groovy friends from CC and Minnesota. This would not have been possible without my parents, Amy and Mark, hands down my favorite people of all time.

7. References

1. Driscoll, C.; Mason, R.; Chan, H.; Jacob, D.; Pirrone, N. Mercury As A Global Pollutant: Sources, Pathways, And Effects. *Environmental Science & Technology* **2013**, *47*, 4967-4983.

2. Environmental Protection Agency. Basic Information about Mercury. https://www.epa.gov/mercury/basic-information-about-mercury (accessed Apr 8, 2019).

3. World Health Organization. Mercury and health. https://www.who.int/news-room/fact-sheets/detail/mercury-and-health (accessed Apr 8, 2019).

4. Selin, N. Global Biogeochemical Cycling Of Mercury: A Review. *Annual Review of Environment and Resources* **2009**, *34*, 43-63.

5. Axelrad, D.; Bellinger, D.; Ryan, L.; Woodruff, T. Dose–Response Relationship Of Prenatal Mercury Exposure And IQ: An Integrative Analysis Of Epidemiologic Data. *Environmental Health Perspectives* **2007**, *115*, 609-615.

6. Hajeb, P.; Jinap, S. Mercury exposure through fish and seafood consumption in the rural and urban coastal communities of Peninsular Malaysia. *World J Fish Marine Sci* **2011**, *3*, 217-226.

7. Guentzel, J.; Portilla, E.; Keith, K.; Keith, E. Mercury Transport And Bioaccumulation In Riverbank Communities Of The Alvarado Lagoon System, Veracruz State, Mexico. *Science of The Total Environment* **2007**, *388*, 316-324.

8. Xu, X.; Newman, M. Mercury Exposure As A Function Of Fish Consumption In Two Asian Communities In Coastal Virginia, USA. *Archives of Environmental Contamination and Toxicology* **2014**, *68*, 462-475.

9. UN Environment. *Global Mercury Assessment 2018*; UN Environment Programme, Chemicals and Health Branch: Geneva, Switzerland, **2019**.

10. Gabriel, M.; Williamson, D.; Zhang, H.; Brooks, S.; Lindberg, S. Diurnal And Seasonal Trends In Total Gaseous Mercury Flux From Three Urban Ground Surfaces. *Atmospheric Environment* **2006**, *40*, 4269-4284.

11. Tewalt, S.; Bragg, L.; Finkelman, R. *Mercury In U.S. Coal; Abundance, Distribution, And Modes Of Occurrence*; Fact Sheet; U.S. Geological Survey, 2001.

12. Zhang, Y.; Jacob, D.; Horowitz, H.; Chen, L.; Amos, H.; Krabbenhoft, D.; Slemr, F.; St. Louis, V.; Sunderland, E. Observed Decrease In Atmospheric Mercury Explained By Global Decline In Anthropogenic Emissions. *Proceedings of the National Academy of Sciences* **2016**, *113*, 526-531.

13. Basic Information about Mercury and Air Toxics Standards https://www.epa.gov/mats/basic-information-about-mercury-and-air-toxics-standards (accessed Mar 10, 2019).

14. Healthier Americans https://www.epa.gov/mats/healthier-americans (accessed Apr 4, 2019).

15. Proposed Revised Supplemental Finding and Results of the Residual Risk and Technology Review https://www.epa.gov/mats/proposed-revised-supplemental-finding-and-results-residual-risk-and-technology-review (accessed Apr 5, 2019).

16. Bade, G. EPA to reconsider rationale for mercury emission rules. https://www.utilitydive.com/news/epa-to-reconsider-rationale-for-mercury-emission-rules/545031/ (accessed Apr 8, 2019).

17. Irfan, U. The EPA Wants To Make It Harder To Ratchet Down Toxic Chemicals From Power Plants. *Vox*, 2018.

18. Liu, B.; Keeler, G.J.; Dvonch, J.T.; Barres, J.A.; Lynam, M.M.; Marsik, F.J.; Taylor-Morgan, J. Temporal variability of mercury speciation in urban air. *Atmospheric Environment* **2007**, *41*, 1911–1923.

19. Nair, U. S.; Wu, Y.; Walters, J.; Jansen, J.; Edgerton, E. S. Diurnal and seasonal variation of mercury species at coastal-suburban, urban, and rural sites in the southeastern United States. *Atmospheric Environment* **2012**, *47*, 499–508.

20. Gratz, L.E.; Keeler, G.J.; Marski, F.J.; Barres, J.A.; Dvonch, J.T. Atmospheric transport of speciated mercury across southern Lake Michigan: Influence from emission sources in the Chicago/Gary urban area. *Scientific Total Environment* **2013**, *448*, 84–95.

21. Liu, B.; Keeler, G.; Timothy Dvonch, J.; Barres, J.; Lynam, M.; Marsik, F.; Morgan, J. Urban–Rural Differences In Atmospheric Mercury Speciation. *Atmospheric Environment* **2010**, *44*, 2013-2023.

22. U.S. Census Bureau QuickFacts: Colorado Springs city, Colorado; United States https://www.census.gov/quickfacts/fact/table/coloradospringscitycolorado,US/PST045217 (accessed Apr 5, 2019).

23. Martin Drake Power Plant. http://www.csu.org/Pages/martin-drake-b.aspx (accessed Apr 5, 2019).

24. U.S. Environmental Protection Agency. Air Markets Program Data (AMPD). Available online: http://ampd.epa.gov/ampd/ (accessed Apr 5, 2019).

25. Nixon Power Plant fire. http://www.csu.org/Pages/nixonfire.aspx (accessed Apr 5, 2019).

26. *U.S. EPA*. 2014 National Emissions Inventory Data. Mercury – 7439976. https://www.epa.gov/air-emissions-inventories/2014-national-emissions-inventory-nei-data (accessed April 4, 2019).

27. About the Refuge. http://www.fws.gov/refuge/Rocky_Flats/about.html (accessed Apr 1, 2019).

28. Steffen, A.; Schroeder, W.; Bottenheim, J.; Narayan, J.; Fuentes, J. Atmospheric mercury concentrations: measurements and profiles near snow and ice surfaces in the Canadian Arctic during Alert 2000. *Atmospheric Environment* **2002**, 36, 2653-2661.

29. Swartzendruber, P.; Chand, D.; Jaffe, D.; Smith, J.; Reidmiller, D.; Gratz, L.; Keeler, J.; Strode, S.; Jaeglé, L.; Talbot, R. Vertical Distribution Of Mercury, CO, Ozone, And Aerosol Scattering Coefficient In The Pacific Northwest During The Spring 2006 INTEX-B Campaign. *Journal of Geophysical Research* **2008**, *113*.

30. McClure, C.; Jaffe, D.; Edgerton, E. Evaluation Of The Kcl Denuder Method For Gaseous Oxidized Mercury Using Hgbr2 At An In-Service Amnet Site. *Environmental Science & Technology* **2014**, *48*, 11437-11444.

31. Rutter, A.; Schauer, J. The Effect Of Temperature On The Gas–Particle Partitioning Of Reactive Mercury In Atmospheric Aerosols. *Atmospheric Environment* **2007**, *41*, 8647-8657.

32. Miller, M.; Dunham-Cheatham, S.; Gustin, M.; Edwards, G. Evaluation of cation exchange membrane performance under exposure to high Hg 0 and HgBr 2 concentrations. *Atmospheric Measurement Techniques* **2019**, *12*, 1207-1217.

33. Obrist, D.; Kirk, J.; Zhang, L.; Sunderland, E.; Jiskra, M.; Selin, N. A Review Of Global Environmental Mercury Processes In Response To Human And Natural Perturbations: Changes Of Emissions, Climate, And Land Use. *Ambio* **2018**, *47*, 116-140.

34. Godish, T. *Air Quality*; 4th ed.; CRC Press: London, **2003**.

35. Lindsey, R. Climate Change: Atmospheric Carbon Dioxide. National Oceanographic and Atmospheric Administration, News & Features. August **2018**. Available online: https://www.climate.gov/news-features/understanding-climate/climate-change-atmospheric-carbon-dioxide (accessed on 8 October 2018).

36. Koerner, B.; Klopatek, J. Anthropogenic And Natural CO_2 Emission Sources In An Arid Urban Environment. *Environmental Pollution* **2002**, *116*, S45-S51.

37. Gratz, L.E.; Jaffe, D.J.; Hee, J.R. Causes of increasing ozone and decreasing carbon monoxide in springtime at the Mt. Bachelor Observatory from 2004 to 2013. *Atmospheric Environment* **2015**, *109*, 323–330.

38. Novelli, P.C.; Masarie, K.A.; Lang, P.M.; Hall, B.M.; Myers, R.C.; Elkins, J.W. Reanalysis of tropospheric CO trends: Effects of the 1997-1998 wildfires. *J. Geophysical Research* **2003**, *108*, 4464.

39. Cole, A.; Steffen, A.; Eckley, C.; Narayan, J.; Pilote, M.; Tordon, R.; Graydon, J.; St. Louis, V.; Xu, X.; Branfireun, B. A Survey Of Mercury In Air And Precipitation Across Canada: Patterns And Trends. *Atmosphere* **2014**, *5*, 635-668.

40. Gratz, L.; Eckley, C.; Schwantes, S.; Mattson, E. Ambient Mercury Observations Near A Coal-Fired Power Plant In A Western U.S. Urban Area. *Atmosphere* **2019**, *10*, 176.

41. Obrist, D.; Faïn, X.; Berger, C. Gaseous Elemental Mercury Emissions And CO_2 Respiration Rates In Terrestrial Soils Under Controlled Aerobic And Anaerobic Laboratory Conditions. *Science of The Total Environment* **2010**, *408*, 1691-1700.

42. Bash, J.; Miller, D. A Note On Elevated Total Gaseous Mercury Concentrations Downwind From An Agriculture Field During Tilling. *Science of The Total Environment* **2007**, *388*, 379-388.

43. Miller, M.B.; Gustin, M.S. Gas-exchange chamber analysis of elemental mercury deposition/emission to alluvium, ore, and mine tailings. *Chemosphere* **2015**, *131*, 209–216.

44. Nriagu, J. Mercury Pollution From The Past Mining Of Gold And Silver In The Americas. *Science of The Total Environment* **1994**, *149*, 167-181.

45. Kellerhals, M.; Beauchamp, S.; Belzer, W.; Blanchard, P.; Froude, F.; Harvey, B.; McDonald, K.; Pilote, M.; Poissant, L.; Puckett, K. et al. Temporal And Spatial Variability Of Total Gaseous Mercury In Canada: Results From The Canadian Atmospheric Mercury Measurement Network (Camnet). *Atmospheric Environment* **2003**, *37*, 1003-1011.

46. Gustin, M.; Amos, H.; Huang, J.; Miller, M.; Heidecorn, K. Measuring And Modeling Mercury In The Atmosphere: A Critical Review. *Atmospheric Chemistry and Physics* **2015**, *15*, 5697-5713.

47. Jaffe, D.; Cooper, O.; Fiore, A.; Henderson, B.; Tonneson, G.; Russell, A.; Henze, D.; Langford, A.; Lin, M.; Moore, T. Scientific Assessment Of Background

Ozone Over The U.S.: Implications For Air Quality Management. *Elementa: Science of the Anthropocene* **2018**, *6*, 56.

48. Abeleira, A.; Pollack, I.; Sive, B.; Zhou, Y.; Fischer, E.; Farmer, D. Source Characterization Of Volatile Organic Compounds In The Colorado Northern Front Range Metropolitan Area During Spring And Summer 2015. *Journal of Geophysical Research: Atmospheres* **2017**, *122*, 3595-3613.

49. Lyman, S.; Jaffe, D. Formation And Fate Of Oxidized Mercury In The Upper Troposphere And Lower Stratosphere. *Nature Geoscience* **2011**, *5*, 114-117.

50. Madsen, P. Peat Bog Records Of Atmospheric Mercury Deposition. *Nature* **1981**, *293*, 127-130.

51. Weiss-Penzias, P.; Gustin, M.; Lyman, S. Observations Of Speciated Atmospheric Mercury At Three Sites In Nevada: Evidence For A Free Tropospheric Source Of Reactive Gaseous Mercury. *Journal of Geophysical Research* **2009**, *114*.

52. Team, E. ESRL Global Monitoring Division—Global Greenhouse Gas Reference Network.